Strain Analysis of Kayo Formation around Teniya-zaki, Okinawa-jima

Bull. Coll. Sci., Univ. Ryukyus, No. 56 : 165−190 (1993)

Strain Analysis of Kayo Formation around Teniya-zaki, Okinawa-jima

Daigoro HAYASHI * and **Sotaro BABA** **

*Department of Marine Sciences, University of the Ryukyus, Okinawa 903-01, Japan
**Department of Earth Science, Ehime University, Matsuyama 790, Japan

Abstract

The Teniya area in Okinawa-jima situated just north to the Kayo area where Hayashi (1988,1989,1992) accomplished the strain analysis. The Kayo Formation around Teniya-zaki strikes generally northeast to southwest and dips to the west. The result of the strain analysis of the area is similar to that performed by Hayashi (1989); the bedding plane has the tendency parallel to the XY plane of the strain ellipsoid. The intensity of strain ϵ_s takes weaker value than that expected from the folding structure developed in the area. The reason is considered to be the competency contrast between quartz grains of strain marker and matrix. As the values of I_{xym} and χ^2 obtained from R_f/ϕ diagram are larger than the critical value of them, we conclude that there was no initial fabrics of quartz grains before deformation.

Introduction

There are many studies using mineral grains as strain marker. Davidson (1983) used feldspar grains as the strain marker and obtained strain ellipse using the three independent methods, the Ramsay's R_f/ϕ method (1967), Dunnet's R_f/ϕ method (1969, 1971) and Elliott's method (1970). He assumed that schistosity plane is coincide with the XY plane of strain ellipsoid and lineation is the direction of X axis. Lacassin *et al.* (1983) used blue-quartz grains as the strain marker to calculate the strain ellipse using the Fry's method (1979). He also assumed for schistosity plane to be the XY plane and for lineation to be the direction of X axis of strain ellipsoid.

Jensen (1984) treated quartz grain as the strain marker to obtain strain ellipse using the R_f/ϕ method. He assumed that schistosity is coincide with the XY plane and lineation is equal to the direction of X axis of strain ellipsoid. He then conducted the Rayleigh test whether the strain marker had preferred orientation or not. Siddans *et al.* (1984) adopted the green spot in pelitic rock as the strain marker to obtain the strain ellipse using the R_f/ϕ method. The strain ellipsoid is constructed with the method developed by Owens (1984) which is derived from the least square method.

Odling (1984) used the quartz grain in quartzo-feldsparthic gneiss as the strain marker. As the shape of quartz grains is different from that of ellipse, he takes six reference lines with 30° intervals each other on the measurement plane. He set up the center of the quartz grains in eye and measured the length of the line which is parallel to the reference line and pass through the center and limited with the quartz grain boundary. He added and averaged the length of all the grains for each reference line. He assumed that the ellipse which is constructed with the averaged length for each direction, is coincide to

Accepted : August 16, 1993
A part of this work was presented at the 100th Annual Meeting of the Geological Society of Japan in Tokyo, April 5, 1993

the strain ellipse. The strain ellipsoid was calculated with the method proposed by Hext (1963). Seno (1992) used the grains (grain species were not written in his paper) within tuff, conglomerate and quartzite as the strain marker to get the strain ellipse using the Fry's method. He assumed that schistosity plane is coincide with the *XY* plane of the strain ellipsoid. He calculated the strain ellipsoid using both the strain ellipses which are obtained from the plane parallel to the schistosity and from the plane perpendicular to the schistosity.

Many of the methods described here used the grains which have similar shape to ellipse such as quartz grain and they obtained the strain ellipse using the R_f/ϕ method or the Fry method. They assumed that the schistosity plane is coincide with the *XY* plane and the lineation is the direction of *X* axis of the strain ellipsoid. The exclusive examples are that done by Siddans *et al.* (1984) used the Owens's method and that done by Odling (1984) used the Hext's method.

Hayashi (1989, 1992) analyzed the strain in the Kayo area using the *SI3* method which is theoretically clear method to construct strain ellipsoid from the strain ellipses on the mutually perpendicular planes. The present paper analyzes the strain in the Teniya area adjacent to the Kayo area using the *SI3* method and the Lisle's θ curve method to judge whether the marker has initial fabric or not.

Geological Setting

The Pre-Tertiary system of Okinawa-jima is called the Kunchan Group excluded the formations distributing around the Motobu Peninsula. The Kunchan Group is constructed by the Nago Formation and Kayo Formation in ascending order. The Nago Formation is mainly composed of phyllites and greenstones, and no fossils have yet been found. Although the age of the Nago Formation is controvertial, Hayashi and Kizaki (1985) considered it from Cretaceous to Paleogene. The Kayo Formation is composed of alternation of sandstone and mudstone. As Nummulites amakusaensis was found from the formation (Suzuki and Ujiié, 1985), the age of the formation is confirmed as middle Eocene. The Kunchan Group is correlated with the Southern zone of the Shimanto Supergroup from the above mentioned evidence (Hayashi and Kizaki, 1985).

The area which is analyzed in the present paper, is the part indicated in Fig. 1 along the eastern side of Okinawa-jima, the shore line from Teniya to Teniya-zaki. The area is composed of flysch type alternation of sandstone and mudstone of the Kayo Formation. Isoclinal folding whose axial plane dips to northwest is severely developed. The indicators of polarity of beds such as cross lamina, trace fossil and outcrop showing that "soft-layer ruptured deposits" (Gireki-sou in Japanese) gouged out sandstone bed are well observed in the flysch type alternation of sandstone and mudstone around Ban-zaki (Fukuda *et al.*, 1978; Hayashi,1988). Hayashi (1988) decided which topping of the beds is normal or reverse by some sedimentary structures in the area around Ban-zaki. On the contrary, in the area around Teniya-zaki we cannot clearly judge the polarity of beds because of the incompleteness of the research performed by one of us, S. Baba. Figures 2 and 3 illustrate the tectonic map of the area and geological profile, respectively.

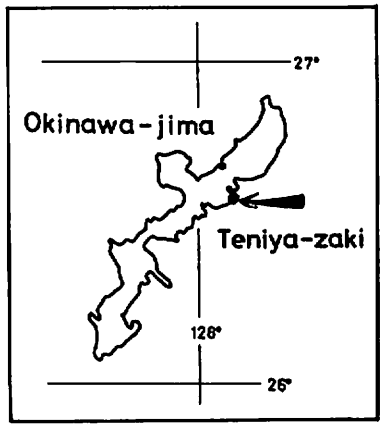

Fig. 1. Index map

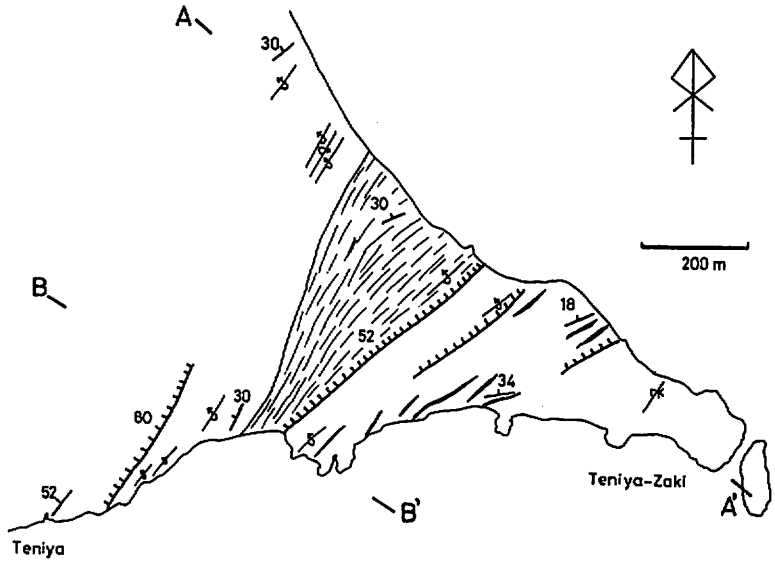

Fig. 2. Tectonic map. Central part hatched with thin short lines is the mudstone dominant alternation of sandstone and mudstone. Solid black thick lines are "soft-layer ruptured deposits". Other white area is composed of the alternation of sandstone and mudstone. AA' and BB' are the lines along which profiles are illustrated in Fig.3.

Fig. 3. Geological profile. Vertical scale is exaggeralated five times of horizontal scale.

Strain Analysis and its Result

Sampling

The oriented rock samples of 47 pieces are collected along the shore line from Teniya to Teniya-zaki in the alternation of sandstone and mudstone. The cubes of which the length of side is about 5 cm are cut from the samples. Three planes sharing a common apex are named as A, B and C plane which are arbitrarily disposed as described in Fig. 4. The intersects of any two planes of the total three planes are defined as x, y and z axis. Here we take z axis as the intersect of B and C planes, and then x and y axes are taken so as to construct a positive coordinate system xyz. If we take xyz system as mentioned a bove, the plane A is always the xy plane and the planes B and C become yz or zx planes. Which plane, B and C, becomes the plane yz or zx depends on the relative spacial disposition of A, B and C

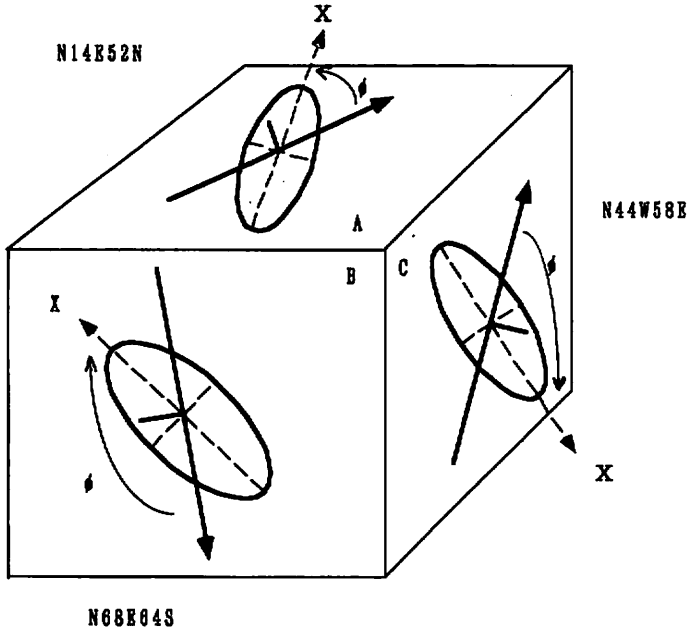

Fig. 4. Cube with three faces A, B and C. Strain ellipse with X and Y axes, and the thick arrow mark indicating strike and dip. The direction of arrow of the strike mark means the "northern direction of strike". ϕ is the angle from the northern direction of strike to the X axis of strain ellipse. The value of ϕ is always taken positive. It is arbitrary to take which faces are A, B or C planes.

planes. Table 1 shows the strike and dip of each sample where xy, yz and zx planes are defined as described above. Table 2 indicates the intersect angle of each two axes, x and y, y and z, and z and x whose value is expected to be 90° , if we take precisely the xyz system orthogonally. Three thin sections are made from each cube of the oriented samples. The total number of thin section is 47 (planes) × 3 (thin sections) =141 pieces. Then micro-photographs are taken from them. We draw 50 to 200 pieces of marker ellipses of quartz grain in each photograph.

The diameter of sand grains of the sandstone is fine (0.1-0.2mm) and occasionally medium. The roundness of sand grains is angular or sub-angular to sub-rounded and the sortness is poor. The mineral assembledge of the sandstone is quartz, plagioclase, K-feldspar,

Table 1. Strike and dip of *xy*, *yz* and *zx* planes.

serial sample number	original sample number	xy plane	yz plane	zx plane
1	1	N85E67N	N16W70S	N36E32S
2	2	N60W83N	N29E77N	N51E19S
3	3	N68W80S	N28E55N	N21E34S
4	3	N62W86N	N34E64S	N22E28N
5	4	N63E70N	N36W82S	N62E22S
6	5	N43W82S	N43E68S	N67E25N
7	6	N86W87S	N 2E43N	N S50W
8	7	N77W88N	N77E 2S	N14E90
9	7	N83W84N	N 5E10N	N33E82S
10	8	N72E75N	N21W85N	N88E12S
11	9	N86W30N	N74W57S	N 9E90
12	10	N62W74N	N39E54S	N15E35N
13	11	N39W81N	N52E82S	N34E21N
14	12	N56W84N	N33E90	N65W 7S
15	13	N65W90	N25E87N	N12E10S
16	16	N34W60N	N78W42S	N45E66N
17	17	N37W89S	N60E52S	N52E35N
18	18	N62E75S	N55W48N	N18W51S
19	20	N82W86S	N16E56N	N 1W30N
20	22	N56E84N	N36W74S	N21W18N
21	23	N74W74S	N20E43N	N 6E40S
22	24	N59W82S	N28E83S	N80W13N
23	25	N17E86N	N73W90	N20E 6S
24	26	N62W74N	N58E29S	N21E66N
25	28	N54W80S	N46E47N	N22E46S
26	29	N77W83S	N21E82S	N43E11N
27	30	N76W86S	N13E80S	N33E 9N
28	35	N48W73N	N42E90	N43W16S
29	36	N38W88N	N61E 4S	N52E85N
30	37	N17W85S	N73E82S	N78E18N
31	38	N50W88S	N38E67N	N48E27S
32	39	N48W90	N38E31S	N42E56N
33	40	N47W87N	N34E28S	N43E67N
34	41	N10W40S	N43W54N	N60E72S
35	42	N12W30S	N46W62N	N53E73S
36	43	N54W85S	N30E48N	N31E50S
37	44	N43W66N	N52E85S	N23W24S
38	45	N36W72N	N84E31S	N44E65N
39	46	N34W68N	N58E86N	N44W21S
40	50	N73W86N	N 8E88N	N12E 8S
41	51	N80W90	N29E43N	N34E48S
42	52	N54W90	N40E50N	N28E32S
43	53	N67W90	N34E 2N	N25E88S
44	54	N63W90	N27E 8N	N30E80S
45	55	N80W58S	N58W40N	N22E75N
46	56	N38W60N	N57E82S	N32W26S
47	57	N52W80N	N40E60N	N48E30S

Table 2. Intersect angle between any two coordinate axes of x, y and *z*.

sample number	x^y °	y^z °	z^x °
1	89.0	88.9	90.6
2	84.9	90.6	89.5
3	91.1	97.9	90.9
4	88.5	90.4	86.3
5	100.4	84.7	88.4
6	88.5	89.5	89.4
7	87.1	89.0	93.6
8	89.5	91.0	89.9
9	91.4	94.8	65.5
10	90.8	94.2	94.8
11	84.2	93.4	88.0
12	92.9	95.9	90.7
13	78.0	92.8	91.3
14	89.3	89.2	88.8
15	83.1	88.4	90.0
16	88.4	92.5	87.2
17	92.8	88.5	83.7
18	87.4	81.4	91.9
19	94.9	89.6	85.9
20	89.2	89.5	92.5
21	97.3	94.8	98.1
22	92.3	88.5	86.6
23	89.8	88.1	89.9
24	90.2	90.4	90.8
25	89.5	86.9	90.1
26	87.7	99.1	91.6
27	92.1	90.4	90.7
28	88.5	91.2	89.9
29	91.2	89.9	90.5
30	79.9	91.3	92.6
31	86.1	87.0	84.2
32	93.4	88.0	89.6
33	85.6	82.7	88.4
34	90.8	91.3	91.2
35	90.4	93.3	91.8
36	82.4	82.0	89.1
37	88.8	91.3	87.6
38	90.3	89.1	92.1
39	90.3	93.5	91.6
40	84.4	81.8	93.8
41	88.7	88.6	86.3
42	97.6	86.2	87.6
43	90.2	92.0	90.1
44	92.3	90.2	87.2
45	94.9	84.6	88.2
46	97.1	93.9	89.2
47	90.0	97.1	94.2

microcline, muscovite, biotite, chlorite, opaque minerals, and rock flakes. The features which indicate any deformation are not seen except that quartz grains show frequently wavy distinction. Biotite is changed almost to chlorite so that biotite is rarely found. The two types of sandstone are recognized, one is wacke and the other is arenite.

Two Dimensional Strain Analysis

The strain ellipses on three section planes A, B and C for each sample are calculated using the *SI* method as shown on Table 3. The *SI* method is the technique to calculate

tectonic strain ellipse developed by Shimamoto and Ikeda (1976). The value of long axis X and short axis Y of strain ellipse are normalized as no volume change ($XY=1$). The parameter R is the axial ratio of strain ellipse ($R=X/Y$) and ϕ is the angle between the direction of X-axis and the northern direction of strike of the plane concerned. The

Table 3. Values of strain ellipse. X : length of long axis of strain ellipse. Y : length of short axis of strain ellipse. R : axial ratio of strain ($\frac{X}{Y}$) . Φ : angle from the northern direction of strike to the X axis of strain.

sample	xy plane				yz plane				zx plane			
number	X	Y	R	Φ °	X	Y	R	Φ °	X	Y	R	Φ °
1	1.20	.83	1.44	43.	1.09	.92	1.19	-32.	1.22	.82	1.48	47.
2	1.15	.87	1.31	44.	1.03	.97	1.06	-79.	1.27	.78	1.63	17.
3	1.08	.92	1.17	62.	1.21	.82	1.47	12.	1.20	.84	1.43	19.
4	1.13	.89	1.27	16.	1.08	.93	1.16	20.	1.15	.87	1.32	29.
5	1.01	.99	1.02	-36.	1.03	.97	1.07	66.	1.12	.89	1.25	13.
6	1.24	.81	1.53	-14.	1.12	.89	1.25	29.	1.21	.83	1.47	23.
7	1.22	.82	1.49	-23.	1.10	.91	1.22	-35.	1.10	.91	1.21	-57.
8	1.20	.83	1.45	39.	1.23	.81	1.51	-35.	1.01	.99	1.02	-21.
9	1.19	.84	1.41	-48.	1.22	.82	1.49	-39.	1.07	.93	1.15	19.
10	1.23	.82	1.50.	22.	1.15	.87	1.33	-24.	1.04	.97	1.07	-55.
11	1.28	.78	1.64	-47.	1.13	.89	1.27	17.	1.07	.93	1.15	-63.
12	1.23	.81	1.51	-13.	1.20	.83	1.44	-10.	1.08	.93	1.17	-15.
13	1.13	.88	1.28	5.	1.32	.76	1.74	-1.	1.06	.95	1.12	71.
14	1.07	.94	1.14	70.	1.33	.75	1.77	9.	1.25	.80	1.56	-73.
15	1.11	.90	1.23	-27.	1.27	.79	1.61	10.	1.16	.86	1.35	21.
16	1.13	.89	1.27	40.	1.16	.86	1.35	22.	1.02	.98	1.05	-77.
17	1.02	.98	1.03	34.	1.09	.92	1.18	-48.	1.07	.94	1.14	-12.
18	1.20	.83	1.45	56.	1.34	.75	1.79	-41.	1.07	.94	1.14	-4.
19	1.08	.92	1.17	49.	1.10	.91	1.22	-4.	1.05	.95	1.10	-27.
20	1.13	.88	1.28	-38.	1.26	.79	1.59	24.	1.11	.90	1.24	-13.
21	1.28	.78	1.63	-20.	1.13	.88	1.28	78.	1.14	.88	1.29	9.
22	1.13	.88	1.29	23.	1.06	.95	1.12	73.	1.10	.91	1.20	-14.
23	1.11	.90	1.23	-14.	1.39	.72	1.94	15.	1.07	.94	1.14	-81.
24	1.14	.87	1.31	68.	1.22	.82	1.49	-23.	1.04	.98	1.08	13.
25	1.07	.94	1.14	7.	1.17	.85	1.37	-3.	1.17	.85	1.37	33.
26	1.20	.83	1.44	21.	1.07	.93	1.15	-56.	1.21	.82	1.47	7.
27	1.13	.88	1.29	37.	1.04	.96	1.08	20.	1.18	.84	1.40	-1.
28	1.07	.93.	1.16	25.	1.17	.86	1.36	18.	1.07	.93	1.15	-78.
29	1.06	.95	1.11	27.	1.15	.87	1.33	10.	1.03	.97	1.06	-17.
30	1.09	.91	1.20	-24.	1.04	.96	1.08	48.	1.16	.86	1.34	30.
31	1.21	.82	1.47	39.	1.08	.93	1.16	-6.	1.24	.81	1.53	13.
32	1.26	.79	1.59	-33.	1.17	.85	1.37	-50.	1.11	.90	1.24	9.
33	1.05	.95	1.11	-9.	1.06	.94	1.12	65.	1.12	.89	1.25	-13.
34	1.03	.97	1.05	-69.	1.11	.90	1.24	-75.	1.08	.93	1.16	24.
35	1.24	.81	1.54	39.	1.02	.98	1.04	72.	1.20	.83	1.44	-12.
36	1.22	.82	1.49	-40.	1.04	.96	1.09	20.	1.13	.88	1.28	2.
37	1.08	.93	1.16	89.	1.09	.92	1.18	7.	1.21	.83	1.46	-73.
38	1.17	.85	1.37	71.	1.20	.83	1.44	-46.	1.05	.95	1.10	-8.
39	1.12	.89	1.26	24.	1.12	.89	1.26	-63.	1.16	.86	1.35	22.
40	1.23	.81	1.52	-10.	1.06	.95	1.12	-44.	1.18	.84	1.40	9.
41	1.23	.81	1.52	-32.	1.23	.81	1.52	9.	1.06	.94	1.13	60.
42	1.14	.88	1.29	-82.	1.14	.88	1.30	11.	1.11	.90	1.23	-15.
43	1.18	.84	1.40	-72.	1.34	.74	1.80	3.	1.01	.99	1.02	-41.
44	1.23	.81	1.52	-76.	1.18	.85	1.40	9.	1.06	.95	1.11	-63.
45	1.22	.82	1.49	-56.	1.08	.93	1.16	87.	1.22	.82	1.49	2.
46	1.36	.73	1.85	3.	1.08	.93	1.17	31.	1.10	.91	1.20	-71.
47	1.19	.84	1.41	-17.	1.02	.98	1.05	88.	1.15	.87	1.32	-19.

northern direction of strike means, for example, if we consider the strike N40° E, there are two directions which the strike indicates, one is N40° E and the other is S40° W. We call N40° E as the northern direction of strike.

Three Dimensional Strain Analysis

The strain ellipsoid is constructed using the *SI3* method from the strain ellipses of three sections in each sample. The *SI3* method is the technique to calculate tectonic strain ellipsoid described by Shimamoto and Ikeda (1976). The values of longest axis X, intermediate axis Y and shortest axis Z are normalized so as to no volume change ($XYZ=1$) as shown on Table 4. Each parameter indicated on Table 4 is defined as follows.

$$R_{xy} = \frac{X}{Y},\quad R_{yz} = \frac{Y}{Z},\quad k = \frac{R_{xy}-1}{R_{yz}-1},\quad d = \sqrt{(R_{xy}-1)^2 + (R_{yz}-1)^2},$$

$$\varepsilon_{12} = \ell_n R_{xy},\quad \varepsilon_{23} = \ell_n R_{yz},\quad k = \frac{\ell_n R_{xy}}{\ell_n R_{yz}},\quad D = \sqrt{(\ell_n R_{xy})^2 + (\ell_n R_{yz})^2},$$

$$\varepsilon_s = \sqrt{\frac{(\ell_n R_{xy})^2 + (\ell_n R_{yz})^2 + (\ell_n R_{zx})^2}{3}},\quad \nu = \frac{1-K}{1+K}$$

Table 4. Values of strain ellipsoid. X: length of long axis of strain ellipsoid. Y: length of intermediate axis of strain ellipsoid. Z: length of short axis of strain ellipsoid. R_{XY}: axial ratio of strain $(\frac{X}{Y})$. R_{YZ}: axial ratio of strain $(\frac{Y}{Z})$. Meanings of the other parameters are referred to text.

sample number	X	Y	Z	Rxy	Ryz	k	d	ε12	ε23	K	D	εs	ν
1	1.369	.910	.803	1.505	1.133	3.803	.522	.408	.125	3.279	.427	.394	-.533
2	1.233	.951	.853	1.297	1.114	2.593	.318	.260	.108	2.399	.282	.268	-.412
3	1.301	.955	.805	1.362	1.187	1.935	.407	.309	.171	1.801	.353	.344	-.286
4	1.155	1.054	.822	1.096	1.283	.339	.299	.091	.249	.367	.265	.249	.463
5	1.071	1.027	.909	1.043	1.130	.334	.137	.042	.122	.348	.129	.121	.484
6	1.327	1.000	.754	1.327	1.326	1.005	.462	.283	.282	1.004	.400	.400	-.002
7	1.220	1.038	.790	1.175	1.314	.558	.359	.161	.273	.591	.317	.311	.257
8	1.337	.971	.770	1.376	1.261	1.442	.458	.319	.232	1.377	.395	.392	-.159
9	1.365	.951	.771	1.436	1.233	1.868	.494	.362	.210	1.725	.418	.408	-.266
10	1.199	1.069	.781	1.121	1.369	.329	.389	.115	.314	.365	.334	.314	.466
11	1.259	1.007	.789	1.250	1.276	.908	.372	.223	.244	.916	.331	.330	.044
12	1.193	1.110	.755	1.074	1.471	.157	.477	.071	.386	.185	.392	.349	.688
13	1.243	1.048	.768	1.186	1.364	.512	.409	.171	.311	.551	.354	.345	.290
14	1.415	.898	.787	1.575	1.142	4.050	.593	.455	.133	3.421	.474	.436	-.548
15	1.302	.975	.788	1.336	1.238	1.404	.411	.289	.214	1.350	.359	.357	-.149
16	1.180	.979	.866	1.206	1.130	1.577	.243	.187	.123	1.526	.224	.220	-.209
17	1.113	.978	.919	1.138	1.064	2.151	.152	.129	.062	2.079	.144	.138	-.350
18	1.284	1.074	.725	1.195	1.483	.405	.521	.179	.394	.453	.433	.414	.376
19	1.129	1.001	.885	1.128	1.132	.966	.184	.120	.124	.968	.173	.173	.016
20	1.240	.967	.834	1.282	1.160	1.762	.325	.249	.149	1.673	.290	.284	-.252
21	1.343	.966	.771	1.391	1.252	1.550	.465	.330	.225	1.467	.399	.395	-.189
22	1.143	.954	.917	1.197	1.041	4.816	.201	.180	.040	4.485	.184	.166	-.635
23	1.350	1.007	.735	1.341	1.370	.920	.503	.293	.315	.931	.430	.430	.038
24	1.182	1.061	.798	1.115	1.330	.348	.349	.109	.285	.381	.305	.286	.448
25	1.276	.921	.851	1.385	1.083	4.612	.394	.325	.080	4.062	.335	.304	-.605
26	1.287	.968	.802	1.329	1.207	1.591	.389	.285	.188	1.513	.341	.337	-.204
27	1.157	1.069	.809	1.083	1.322	.257	.332	.080	.279	.285	.290	.266	.556
28	1.226	.957	.852	1.281	1.123	2.274	.306	.247	.116	2.126	.273	.263	-.360
29	1.153	.974	.891	1.184	1.093	1.969	.208	.169	.089	1.890	.191	.185	-.308
30	1.144	1.045	.837	1.095	1.248	.383	.266	.091	.222	.410	.240	.227	.419
31	1.214	1.070	.770	1.135	1.389	.347	.412	.127	.329	.385	.352	.333	.444
32	1.194	1.074	.780	1.112	1.377	.297	.393	.106	.320	.332	.337	.314	.502
33	1.158	.944	.914	1.226	1.033	6.936	.229	.204	.032	6.354	.207	.181	-.728
34	1.143	.988	.886	1.157	1.115	1.373	.195	.146	.109	1.346	.182	.181	-.148
35	1.365	.872	.840	1.564	1.039	14.548	.565	.447	.038	11.758	.449	.382	-.843
36	1.197	1.008	.829	1.188	1.216	.872	.286	.172	.195	.883	.260	.260	.052
37	1.228	1.000	.814	1.228	1.228	1.004	.322	.206	.205	1.004	.290	.290	-.002
38	1.170	1.077	.793	1.086	1.359	.241	.369	.083	.306	.271	.317	.290	.574
39	1.166	1.073	.799	1.087	1.342	.253	.353	.083	.294	.282	.306	.280	.560
40	1.201	1.052	.792	1.142	1.328	.432	.367	.132	.284	.467	.313	.301	.384
41	1.391	.687	.811	1.569	1.093	6.098	.577	.451	.089	5.049	.459	.409	-.669
42	1.233	.982	.826	1.256	1.189	1.351	.318	.228	.173	1.314	.286	.285	-.136
43	1.230	1.103	.737	1.115	1.495	.232	.509	.109	.402	.270	.417	.381	.574
44	1.354	.908	.814	1.492	1.116	4.256	.505	.400	.109	3.658	.415	.379	-.571
45	1.298	1.021	.755	1.272	1.352	.772	.445	.240	.302	.797	.385	.384	.113
46	1.246	1.071	.749	1.163	1.430	.378	.460	.151	.358	.421	.388	.369	.407
47	1.130	.953	.929	1.186	1.025	7.434	.188	.171	.025	6.903	.172	.150	-.747

The Flinn diagram is shown in Fig. 5. We can say from the figure,

(1) The maximum value of strain intensity d is 0.6 and take the value ranging 0.3 to 0.4 frequently. These values indicate that the deformation of the area was weaker than the other folded area, for example, the Alps.

(2) The number of stain ellipsoid which belongs to the prolate type is 25 and that of oblate type is 22. As they are roughly the same number, we cannot say which type of deformation was dominant in the area.

The distribution of principal axes of strain ellipsoid is drawn as the lower hemisphere projection on to the Schmidt net in Fig. 6. We collect so many samples in the area A and B that we draw the distribution of principal axes in the separate sheets, that is, in Fig. 7 for the area A and in Fig. 8 for the area B. The distribution of Z-axis of all the strain

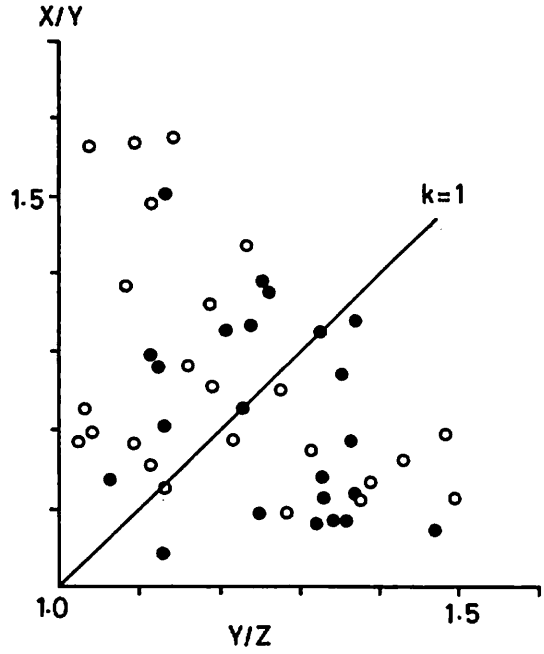

Fig. 5. Flinn diagram. Open circle : samples collected from hinge part, Solid circle : samples collected from limb part

ellipsoids is illustrated in Fig. 9. As the Z-axes are seen randomly distributed, we consider that there are no tendencies about the direction of Z-axes which are not classified but as a whole. Table 5 indicates the intersect angle of every two principal strain axes, X and Y, Y and Z, and Z and X. The angle value exceeding 10° difference from 90° is seen in the sample 9 (intersect angle between Z and X =78.1°) and sample 13 (intersect angle between Y and Z =78.9°). We think that the wobble of intersect angle depends on the incomplete orthogonal coordinate system xyz. In fact the intersect angle of z and x with regard to the sample 9 is 65.5° and that of x and y for sample 13 is 78.0°, which must be 90° if the xyz system is orthogonal.

Index of Symmetry

As the strain marker is the quartz grain of sedimentary rock, there is a possibility that the strain marker has an initial foliation, in other words initial preferred orientation. We know whether the strain marker has a preferred foliation or not, by examining the symmetry of the R_f/ϕ diagram (Lisle, 1985). The symmetry is described by the "index of symmetry" (abbreviated it as I_{sym} hereafter). Table 6 shows the values of I_{sym} calculated on each section plane of the samples. As many values of I_{sym} are over 0.8 in Table 6, we conclude that initial markers of quartz grain are randomly oriented. In order to perform more detail discussion, we use Table 4.1 of Lisle's book (Lisle, 1985, p.15). Lisle calculated the values of I_{sym} where he changed intensity of tectonic strain 1.5, 2.0, 3.0, 5.0 and 10.0, and changed the sample size 20, 35, 60, 100 and 200 where initial markers are randomly distributed. He obtained the critical values of I_{sym} for 5% and 10% of the level of significance. For example, with regard to the tectonic strain $R=1.5$

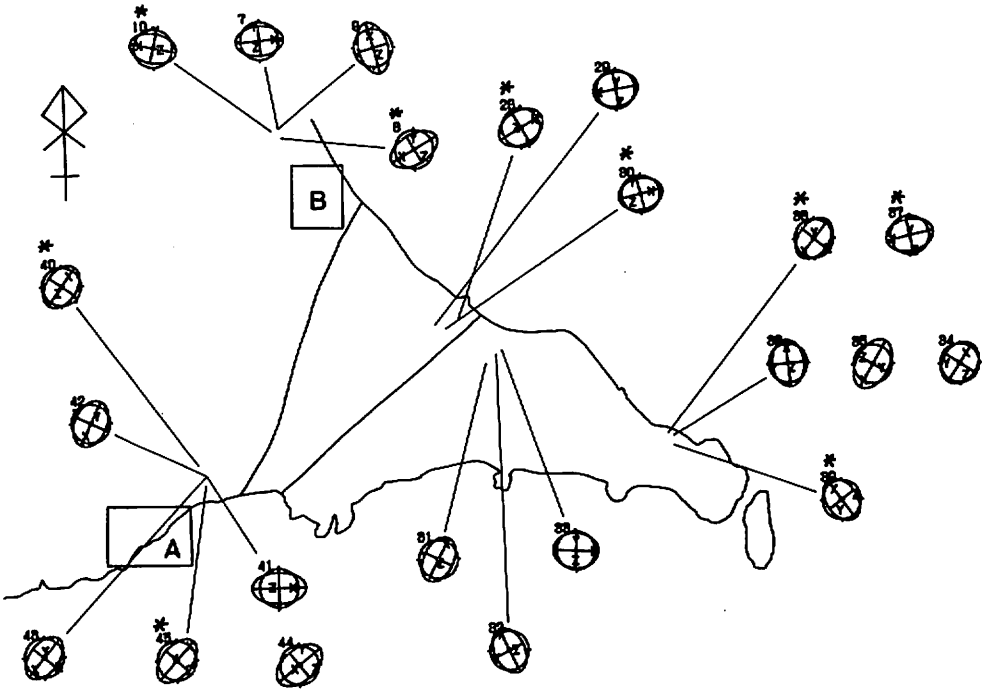

Fig. 6. Distribution of strain ellipsoid. Circle is the Schmidt net. *X*, *Y* and *Z* are the principal strain axes projected on the lower hemisphere of the net. Ellipse represents the *XZ* section of strain ellipsoid. * means the sample collected from limb part. The areas A and B are illustrated on the separate figures because of their large number of samples.

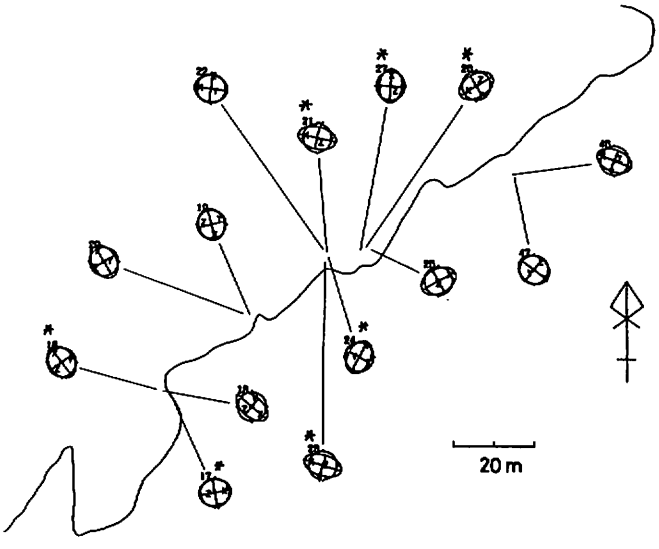

Fig. 7. Distribution of strain ellipsoid in the area A. Other explanations are same as in Fig. 6.

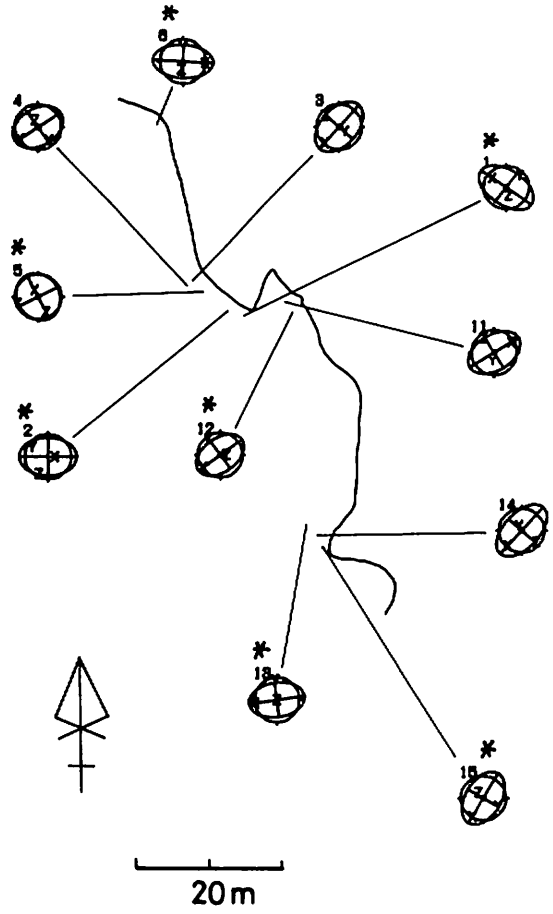

Fig. 8. Distribution of strain ellipsoid in the area B. Other explanations are same as in Fig. 6.

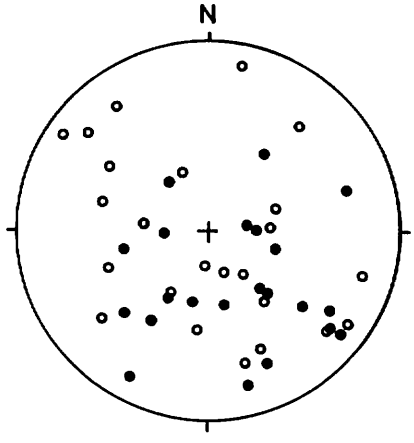

Fig. 9. *Z* axes of 47 strain ellipsoids projected on the lower hemisphere of the Schmidt net. Solid circle : sample collected from limb part, Open circle : sample collected from hinge part.

Table 5. Intersect angle between any two principal strain axes of *X*, *Y* and *Z*.

sample number	X^Y °	Y^Z °	Z^X °
1	89.8	88.6	90.7
2	88.3	90.8	89.0
3	94.0	93.1	94.6
4	91.3	87.9	87.8
5	98.8	85.7	86.1
6	89.1	88.8	90.1
7	92.9	90.3	87.3
8	89.2	91.3	90.2
9	93.6	91.4	78.1
10	94.3	92.2	92.3
11	94.1	89.9	89.9
12	87.9	89.4	96.1
13	93.7	78.9	86.9
14	88.5	89.6	88.9
15	89.9	84.9	87.3
16	91.5	88.9	86.4
17	94.6	90.5	85.9
18	87.7	83.1	93.9
19	88.3	93.5	88.2
20	91.0	89.7	88.1
21	91.3	99.2	95.4
22	91.7	88.0	88.1
23	90.0	89.8	89.2
24	90.1	90.3	90.5
25	88.1	88.3	87.7
26	89.0	93.6	93.8
27	91.7	90.8	90.4
28	90.6	88.4	90.0
29	90.6	90.9	90.2
30	84.4	81.9	91.0
31	87.4	87.8	85.5
32	91.0	88.3	89.5
33	84.4	88.9	85.4
34	92.0	90.7	90.0
35	90.0	93.1	88.7
36	88.4	80.4	88.8
37	89.4	89.0	88.5
38	92.1	90.4	88.8
39	90.9	88.7	88.6
40	87.2	84.0	96.3
41	90.6	86.6	90.3
42	85.3	89.3	88.4
43	89.6	91.1	91.0
44	89.6	87.6	90.3
45	90.9	92.3	85.1
46	89.7	89.3	97.9
47	91.6	93.7	93.7

and the sample size $n=100$ in the level of significance 5%, we find out a critical value of I_{sym} 0.74. This means that we have one chance to get the value under 0.74 of I_{sym} in total 20 challenges and therefore we judge that this case will happen rarely. We deduce that if the value of I_{sym} is over 0.74, the direction of long axis of initial markers is randomly distributed in the level of significance 5%. This means that there were no initial fabrics in the area concerned. The critical value of I_{sym} for $R=1.5$ is 0.6 (sample size $n=60$, 5% L.O.S.=level of significance) and 0.74 (n=100, 5% L.O.S.) from the Lisle's Table 4.1. We have a plane where the value of I_{sym} is under the critical value, that is, we are better to throw away the strain analysis on the plane because there was initial fabric on the plane. The plane fit to the case is 43-*xy* ($n=74$, $I_{sym}=0.65$). In the condition $R\rangle$ 1.5, we have 22 planes as follows. 6-*xy* ($R=1.53$, $n=39$, $I_{sym}=0.92$), 11-*xy* ($R=1.64$, $n=68$, $I_{sym}=0.94$), 12-*xy* ($R=1.51$, $n=71$, $I_{sym}=0.93$), 21-*xy* (the values of *R*, *n* and I_{sym} are referred to Table 6, hereafter), 32-*xy*, 35-*xy*, 40-*xy*, 41-*xy*, 44-*xy*,

46-*xy*, 8-*yz*, 13-*yz*, 14-*yz*, 15-*yz*, 18-*yz*, 20-*yz*, 23-*yz*, 41-*yz*, 43-*yz*, 2-*zx*, 14-*zx* and 31-*zx*. As the critical value of I_{sym} for $R=2.0$ is 0.73 ($n=60$, 5% L.O.S.) and 0.80 ($n=100$, 5% L.O.S.), the values of I_{sym} of 22 planes are higher than the critical value. Therefore, there were no initial fabrics on the 22 planes.

Initial Maker Ellipse

The initial marker ellipses are restored from both the marker ellipses and the strain ellipse for each plane. The important parameters are also shown on Table 6. The parameters R and ϕ are the axial ratio of strain ellipse obtained with *SI* method and the angle of long axis of the strain ellipse from the reference line. The parameter ϕ is the angle of the long axis of the strain ellipse obtained with the R_f/ϕ method (vector mean of angle of all the points in each R_f/ϕ diagram) from the reference line. The parameter I_{sym} is the symmetric index and the "size" is the number of measurement. The parameters ν, R_s, $\chi^2\phi$ and $\chi^2\theta$ are the degree of freedom, axial ratio of strain ellipse obtained with the θ curve method by Lisle (1985), χ^2-value at the R_f/ϕ diagram and χ^2-value at the R_i/θ diagram, respectively. The values of $\chi^2\phi$ and $\chi^2\theta$ are calculated using the FORTRAN program developed by Peach and Lisle (1979). As the values of axial ratio of strain obtained from the samples in the area are almost under the value 1.5, we do not recognize significant changes on the feature and distribution of the strain markers of many samples before and after deformation.

Figure 10 indicates the frequency graph of the axial ratio of initial marker ellipse R_i. Figure 11 illustrates the rose diagram of the angle θ between long axis of initial marker ellipse and the reference line where *xy*, *yz* and *zx* planes are arranged from the left hand side to the right. The frequency diagram of R_i is shown in Fig. 10 where the values of R_i are calculated for the divided 40 parts of 0.1 intervals throughout the range 1.0 to 5.0. The number of marker is represented by the percentage of the total number of marker. The percentage value is plotted as the frequency on ordinate where one twentieth of the length of abscissa becomes 1 %. Figure 10 shows that the distribution of R_i of many samples forms a cluster between 1.0 to 2.0. The direction of long axis of initial marker ellipses is represented on the range between 0° to 180° in Fig. 11. The number of the direction of long axis is counted for the 18 parts of each 10° intervals and is described in the form of percent of the total number of marker. The percentage number is plotted as the frequency for every direction as the length of 1 % becomes one fortieth of the diameter of circle.

The frequency diagram of R_i in the area A is shown in Fig. 12 and the rose diagram of long axis of initial marker ellipse in the area A is drawn in Fig. 13. The frequency diagram of R_i and the rose diagram of long axis of initial marker ellipse with regard to the area B are illustrated in Figs. 14 and 15, respectively.

Table 7 shows the parameters, "*str*", ϕ_{mean}, θ_{mean}, R_{fhm} and R_{ihm}, and they mean except for "*str*", the vector mean angle of ϕ, vector mean angle of θ, harmonic mean of R_f and R_i, respectively. The parameter "*str*" is the northern direction of strike of before deformation measured from the direction of the strike after deformation. The R_f/ϕ and R_i/θ diagrams are drawn using the parameters described on Table 7. We decide not to show the diagrams R_f/ϕ and Ri/θ because it gives no profit to us.

Table 6. Results of two dimensional strain analysis. Angles are taken anticlockwise as positive. R : axial ratio of strain ellipse calculated with SI method. Φ : angle measured from the northern direction of strike of after deformation to the X axis of strain ellipse calculated with SI method. ϕ : vector mean of all the data points in the R_f/ϕ diagram. The angle ϕ takes ideally the same value of Φ. I_{sym} : index of symmetry after Lisle. *size* : sample size. ν : degree of freedom in the θ curve method. R_s : axial ratio of strain ellipse obtained with the θ curve method. $\chi^2\phi$: χ^2 value calculated from the R_f/ϕ diagram. $\chi^2\theta$: χ^2 value calculated from the R_s/θ diagram.

sample number	xy plane								
	R	Φ°	φ°	Isym	size	ν	Rs	χ²φ	χ²θ
1	1.44	43.	46.	.81	64	7	1.59	2.88	5.06
2	1.31	44.	50.	.77	57	7	1.39	9.14	8.79
3	1.17	62.	59.	.94	53	7	1.18	3.04	4.17
4	1.27	18.	16.	.88	68	7	1.35	7.00	2.88
5	1.02	-38.	-47.	.92	61	7	1.01	11.95	12.93
6	1.53	-14.	-15.	.92	39	1	1.62	2.54	2.33
7	1.49	-23.	-24.	.90	62	7	1.66	5.32	6.07
8	1.45	39.	39.	.86	56	7	1.66	2.57	1.86
9	1.41	-48.	-48.	.88	86	7	1.50	4.93	4.23
10	1.50	22.	22.	.83	70	7	1.65	4.57	7.14
11	1.64	-47.	-62.	.94	68	7	1.27	4.06	5.53
12	1.51	-13.	-15.	.93	71	7	1.67	6.49	5.76
13	1.28	5.	5.	.94	79	7	1.32	6.95	8.98
14	1.14	70.	64.	.87	83	7	1.19	2.66	5.80
15	1.23	-27.	-26.	.90	91	7	1.25	6.69	3.40
16	1.27	40.	38.	.88	66	7	1.32	8.55	7.03
17	1.03	34.	34.	.93	58	7	1.04	1.65	6.14
18	1.45	56.	53.	.82	56	7	1.55	11.50	6.86
19	1.17	49.	51.	.71	62	7	1.33	2.84	3.81
20	1.28	-38.	-39.	.92	78	7	1.52	6.10	11.49
21	1.63	-20.	-18.	.71	56	7	1.60	14.36	14.36
22	1.29	23.	25.	.91	75	7	1.48	8.87	5.40
23	1.23	-14.	-13.	.90	69	7	1.24	7.09	7.38
24	1.31	68.	69.	.88	66	7	1.32	4.61	6.42
25	1.14	7.	6.	.91	66	7	1.09	3.70	4.61
26	1.44	21.	22.	.94	53	7	1.48	10.21	10.96
27	1.29	37.	36.	.76	63	7	1.39	.97	2.87
28	1.16	25.	24.	.93	60	7	1.12	3.50	8.00
29	1.11	27.	28.	.88	59	7	1.08	5.91	4.90
30	1.20	-24.	-24.	.85	54	7	1.20	3.41	6.00
31	1.47	39.	39.	.93	45	1	1.57	.24	.60
32	1.59	-33.	-33.	.96	46	1	1.70	.78	.26
33	1.11	-9.	-7.	.92	37	1	1.09	2.03	3.32
34	1.05	-69.	77.	.79	48	1	1.04	2.50	.50
35	1.54	39.	41.	.78	69	7	1.50	9.70	13.17
36	1.49	-40.	-40.	.94	70	7	1.54	3.43	3.71
37	1.16	89.	-85.	.73	77	7	1.17	11.44	10.14
38	1.37	71.	72.	.91	64	7	1.39	5.69	5.69
39	1.26	24.	24.	.94	62	7	1.32	2.52	4.45
40	1.52	-10.	-13.	.93	54	7	1.70	3.41	3.78
41	1.52	-32.	-32.	.93	93	7	1.69	13.34	9.47
42	1.29	-82.	-84.	.87	90	7	1.37	6.89	4.22
43	1.40	-72.	-69.	.65	74	7	1.44	14.38	17.08
44	1.52	-76.	-77.	.95	105	7	1.50	9.00	6.33
45	1.49	-56.	-54.	.95	80	7	1.51	7.75	9.00
46	1.85	3.	4.	.94	66	7	1.93	5.82	8.55
47	1.41	-17.	-13.	.63	63	7	1.38	8.90	6.68

sample number	yz plane								
	R	Φ°	φ°	Isym	size	ν	Rs	χ²φ	χ²θ
1	1.19	-32.	-36.	.78	74	7	1.16	4.92	4.11
2	1.05	-79.	-66.	.96	54	7	1.10	8.22	11.93
3	1.47	12.	12.	.95	80	7	1.55	9.50	10.75

4	1.16	20.	20.	.93	75	7	1.17	5.40	3.00
5	1.07	66.	63.	.98	49	1	1.04	.55	1.86
6	1.25	29.	26.	.93	54	7	1.26	7.11	11.19
7	1.22	-35.	-37.	.83	70	7	1.19	4.57	3.43
8	1.51	-35.	-35.	.87	62	7	1.65	5.42	4.77
9	1.49	-39.	-38.	.92	78	7	1.58	4.82	3.54
10	1.33	-24.	-27.	.91	70	7	1.39	5.43	6.00
11	1.27	17.	19.	.91	66	7	1.47	9.45	10.97
12	1.44	-10.	-7.	.88	80	7	1.41	10.00	12.75
13	1.74	-1.	-1.	.99	83	7	1.89	11.58	9.65
14	1.77	9.	9.	.96	73	7	1.83	8.51	3.03
15	1.61	10.	9.	.79	79	7	1.64	7.71	8.22
16	1.35	22.	21.	.93	69	7	1.40	7.09	6.22
17	1.18	-48.	-50.	.96	46	1	1.16	.44	.78
18	1.79	-41.	-41.	.83	60	7	1.95	4.00	4.33
19	1.22	-4.	-6.	.97	60	7	1.14	5.00	3.00
20	1.59	24.	25.	.85	54	7	1.67	9.33	4.89
21	1.28	78.	75.	.96	75	7	1.32	7.53	9.13
22	1.12	73.	80.	.94	66	7	1.03	10.67	16.73
23	1.94	15.	15.	.94	51	7	2.08	4.10	4.88
24	1.49	-23.	-23.	.97	78	7	1.56	6.36	9.95
25	1.37	-3.	-5.	.93	54	7	1.49	8.59	9.70
26	1.15	-56.	-54.	.90	60	7	1.14	9.00	11.33
27	1.08	20.	0.	.75	72	7	1.03	4.94	9.39
28	1.36	18.	12.	.70	69	7	1.22	7.96	7.09
29	1.33	10.	9.	.98	53	7	1.34	2.28	3.79
30	1.08	48.	42.	.89	36	1	1.24	1.56	2.00
31	1.16	-6.	-6.	.81	59	7	1.11	9.64	14.73
32	1.37	-50.	-48.	.92	37	1	1.44	1.16	1.38
33	1.12	65.	59.	.93	43	1	1.07	1.37	2.12
34	1.24	-75.	-75.	.93	60	7	1.32	12.33	5.00
35	1.04	72.	80.	.98	61	7	1.09	5.07	6.70
36	1.09	20.	11.	.77	57	7	1.09	5.63	4.93
37	1.18	7.	9.	.83	65	7	1.11	4.08	5.00
38	1.44	-46.	-46.	.89	70	7	1.56	6.00	8.00
39	1.26	-63.	-64.	.84	64	7	1.20	8.50	5.69
40	1.12	-44.	-42.	.82	78	7	1.09	6.61	5.59
41	1.52	9.	7.	.67	75	7	1.42	20.07	24.87
42	1.30	11.	10.	.87	62	7	1.23	8.00	6.71
43	1.80	3.	3.	.90	80	7	1.90	6.25	6.75
44	1.40	9.	8.	.99	79	7	1.61	6.19	5.68
45	1.16	87.	86.	.92	72	7	1.15	4.11	5.50
46	1.17	31.	35.	.94	72	7	1.16	3.00	6.61
47	1.05	88.	59.	.80	90	7	1.00	6.67	8.44

sample	zx plane								
number	R	Φ°	ϕ°	I_{sym}	size	ν	R_s	$\chi^2\phi$	$\chi^2\theta$
1	1.48	47.	47.	.81	69	7	1.57	12.01	8.83
2	1.63	17.	19.	.72	53	7	1.79	7.57	7.19
3	1.43	19.	19.	.93	60	7	1.51	9.00	8.00
4	1.32	29.	29.	.97	62	7	1.27	6.07	7.03
5	1.25	13.	15.	.78	59	7	1.25	9.98	14.05
6	1.47	23.	24.	.90	60	7	1.55	6.00	12.67
7	1.21	-57.	-54.	.85	59	7	1.28	8.97	15.41
8	1.02	-21.	-11.	.97	60	7	1.03	9.33	15.00
9	1.15	19.	16.	.88	68	7	1.04	9.06	9.65
10	1.07	-55.	-46.	.86	72	7	1.01	11.33	13.56
11	1.15	-63.	-63.	.90	78	7	1.12	8.67	13.28
12	1.17	-15.	-12.	1.00	68	7	1.14	5.24	4.06

13	1.12	71.	75.	.99	79	7	1.13	9.23	9.23
14	1.56	-73.	-72.	.85	89	7	1.58	3.02	3.25
15	1.35	21.	22.	.94	72	7	1.40	2.72	3.28
16	1.05	-77.	-75.	.90	69	7	1.07	1.29	1.29
17	1.14	-12.	-11.	.89	56	7	1.25	7.21	9.00
18	1.14	-4.	-1.	.84	74	7	1.10	3.30	3.84
19	1.10	-27.	-22.	.92	72	7	1.14	6.06	10.22
20	1.24	-13.	-14.	.81	54	7	1.28	4.52	5.63
21	1.29	9.	9.	.98	63	7	1.19	5.41	7.00
22	1.20	-14.	-20.	.78	64	7	1.31	4.44	4.75
23	1.14	-81.	-81.	.82	63	7	1.19	2.87	3.19
24	1.08	13.	16.	.95	57	7	1.14	4.23	5.98
25	1.37	33.	34.	.89	56	7	1.42	7.93	6.86
26	1.47	7.	5.	.74	49	1	1.36	1.69	3.16
27	1.40	-1.	0.	.85	61	7	1.50	1.79	4.41
28	1.15	-78.	-76.	.87	53	7	1.15	2.28	1.91
29	1.06	-17.	-22.	.95	67	7	1.01	4.19	5.69
30	1.34	30.	30.	.96	52	7	1.50	4.15	2.23
31	1.53	13.	13.	1.00	42	1	1.64	.48	.48
32	1.24	9.	9.	.93	41	1	1.38	.27	1.24
33	1.25	-13.	-15.	.93	41	1	1.26	2.61	.27
34	1.16	24.	34.	.71	45	1	1.03	1.84	.60
35	1.44	-12.	-11.	.98	63	7	1.49	4.46	5.09
36	1.28	2.	1.	.86	70	7	1.34	6.29	14.00
37	1.46	-73.	-73.	.94	62	7	1.63	5.10	3.48
38	1.10	-8.	-9.	.91	57	7	1.05	17.56	14.05
39	1.35	22.	19.	.79	71	7	1.36	4.07	5.48
40	1.40	9.	11.	.93	80	7	1.48	10.75	11.25
41	1.13	60.	62.	.99	65	7	1.07	5.00	2.85
42	1.23	-15.	-16.	.89	74	7	1.32	4.38	7.62
43	1.02	-41.	-29.	.97	78	7	1.07	5.59	8.92
44	1.11	-63.	-65.	.90	60	7	1.11	4.00	8.00
45	1.49	2.	2.	.96	90	7.	1.46	11.56	14.22
46	1.20	-71.	-72.	.96	73	7	1.21	5.22	7.96
47	1.32	-19.	-22.	.94	91	7	1.32	8.01	6.03

Averaged Initial Ellipse

According to Shimamoto and Ikeda (1976), the closer the axial ratio $\acute{R}_i$ of averaged initial ellipse is to be unity, the more precise the strain analysis (axial ratio of tectonic strain R, angle between the long axis of strain ellipse and the reference line α) is. The closer the absolute value of angle $|\acute{\theta}-\alpha|$ between the direction α of long axis X of strain ellipse and the direction θ of long axis of the averaged initial ellipse, the more precise the strain analysis (R, α) with regard to the same value $\acute{R}_i$, Table 8 shows the values of $\acute{R}_i$ *and* $|\acute{\theta}-\alpha|$ (indicated as ϕ in Table 8) of the samples in the present area. The many values R_i are close to 1.000 where the deflection from the value 1.000 is the order of 0.001. It means that the value of strain axial ratio R is precise enough in the practical sense.

Figure 16 shows the graph of $\acute{R}_i$ and the sample size. Although Shimamoto and Ikeda (1976) said that the negative relation between $\acute{R}_i$ and sample size was expected, we recognize no clear relationships between them.

Foliation and XY Plane of Strain Ellipsoid

The bedding foliation at the sampling point and the XY plane of strain ellipsoid calculated from the collected samples are drawn as great circles of lower hemisphere projection on the Schmidt net in Fig. 17 with regard to the whole area. The same kind

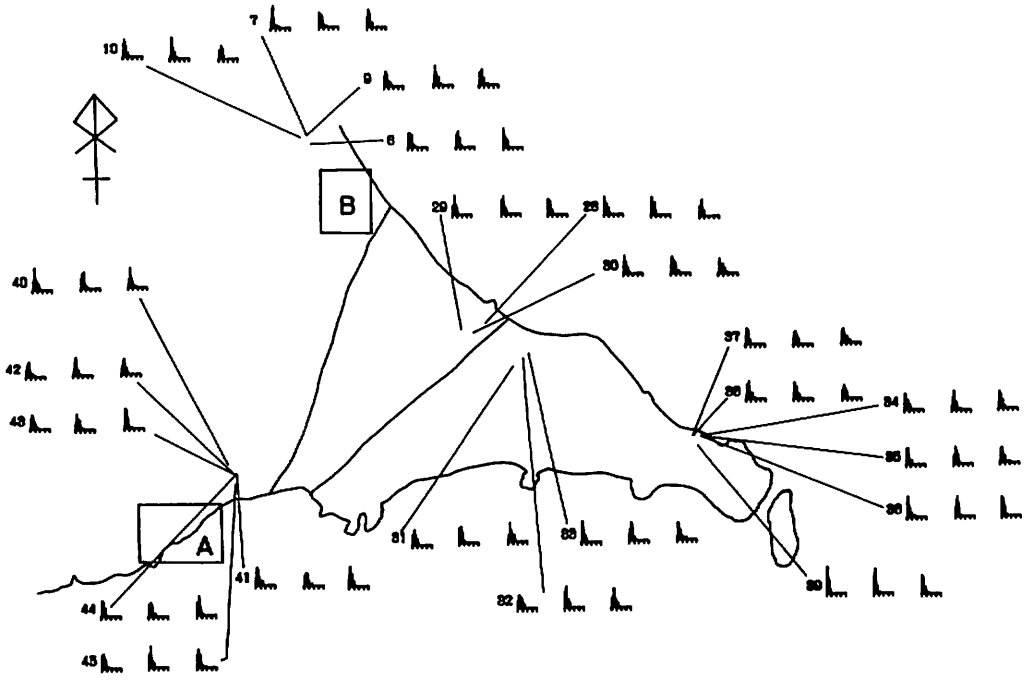

Fig. 10. Distribution map of the frequency diagram of R_i. The value of R_i plots on the abscissa and that of frequency plots on the ordinate. The ticks of the abscissa indicate the values 1, 2, 3, 4 and 5 of R_i from left handside to right. The frequency diagrams are arranged in the order *xy*, *yz* and *zx* planes from left to right. The number attached to the top of the diagram is the sample number.

of Schmidt diagram where great circles are drawn are illustrated in Fig. 18 for the area A and in Fig. 19 for the area B. Three figures show that the foliation measured at the sample collected point is roughly parallel to the *XY* plane of strain ellipsoid obtained at the same collected point.

Conclusions

We conclude about the reliability of the strain analysis as follows.

(1) Was there any initial fabric of strain marker?

It seems that the strain markers were randomly distributed from the rose diagram of the direction of the long axis of initial strain marker. The randomness of strain markers is also recognized from the value of I_{nm} *on the* R_f/ϕ diagram and the larger values of $\chi^2\phi$ than the critical value.

(2) As the value R_i of averaged initial ellipse is very close to 1.0, the precision of strain R is good enough.

We summerize the main features of the present strain analysis as follows.

(1) Hayashi (1988,1989) resulted that the bedding plane was almost parallel to the *XY* plane of strain ellipsoid in Kayo area which lies just to the south of the present area. The result of the present analysis shows the same tendency to that of the Kayo area.

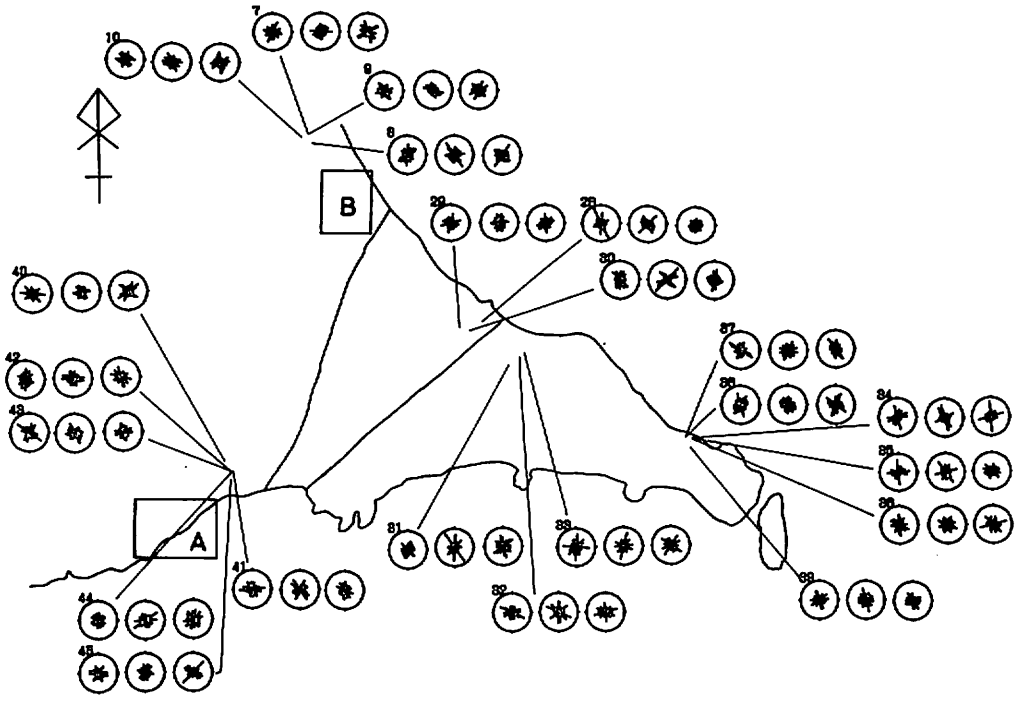

Fig. 11. Distribution map of the rose diagram of θ. Other explanations are same as in Fig. 10.

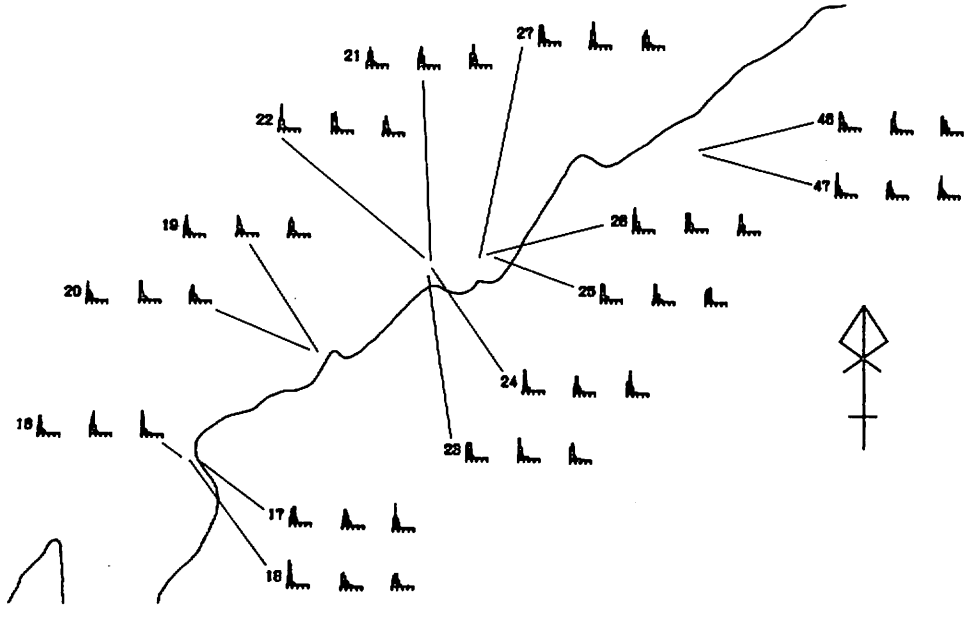

Fig. 12. Distribution map of the frequency diagram of R_i in the area A. Other explanations are same as in Fig. 10.

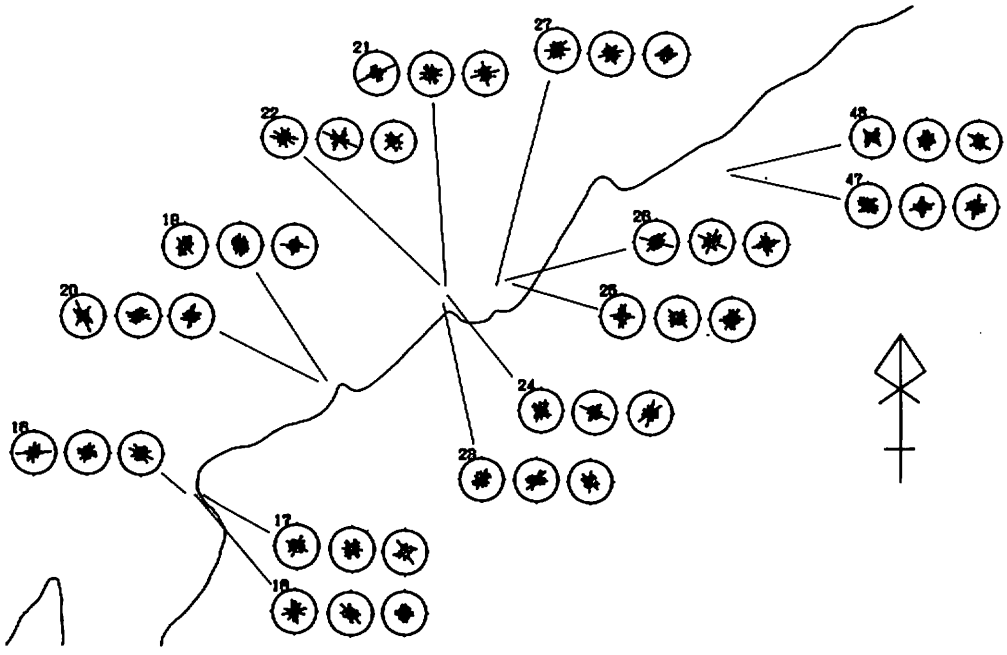

Fig. 13. Distribution map of the rose diagram of θ in the area A. Other explanations are same as in Fig. 10.

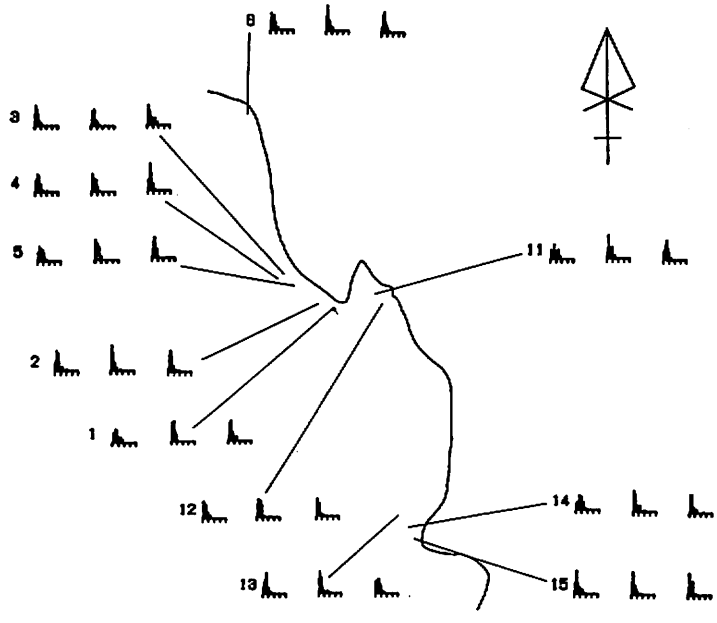

Fig. 14. Distribution map of the frequency diagram of R_i in the area B. Other explanations are same as in Fig. 10.

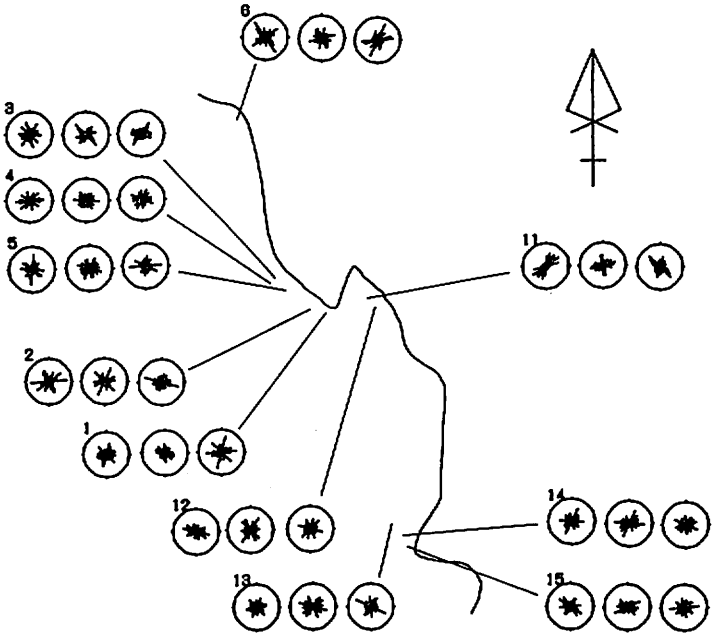

Fig. 15. Distribution map of the rose diagram of θ in the area B. Other explanations are same as in Fig. 10.

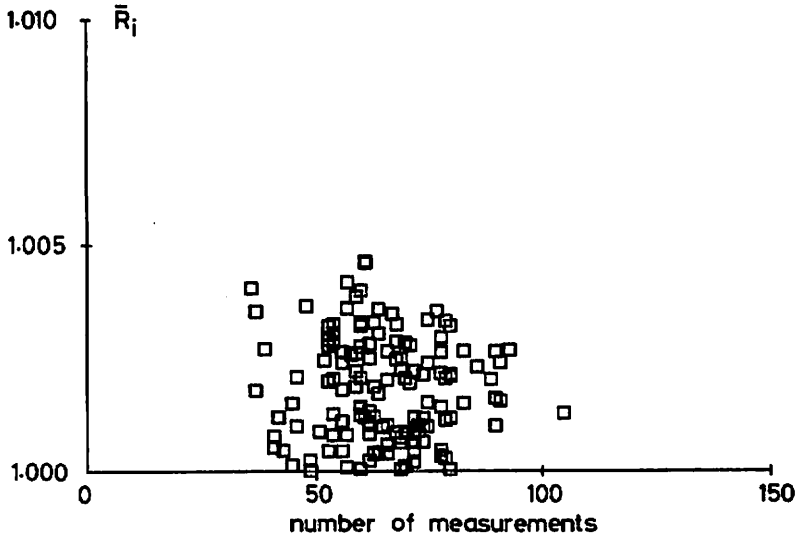

Fig. 16. Diagram of the axial ratio $\bar{R}_i$ of averaged initial ellipse and the sample size. The total plotted number of the averaged initial ellipses is 47 × 3 = 141

Table 7. Index values in the R_f/ϕ and R_i/θ diagram. The angles indicated hereafter are measured from the northern direction of strike of after deformation. Angles are taken anticlockwise as poslitive. *str* : northern direction of strike of before deformation. ϕ_{mean} : vector mean of ϕ. R_{fhm} : harmonic mean of R_f. θ_{mean} : vector mean of θ. R_{ihm} : harmonic mean of R_i.

sample number	xy plane				
	str°	ϕmean°	Rfhm	θmean°	Rihm
1	-10.	46.	1.84	56.	1.63
2	-8.	50.	1.64	48.	1.51
3	-4.	59.	1.43	54.	1.37
4	-4.	16.	1.60	15.	1.49
5	1.	-47.	1.56	-49.	1.55
6	7.	-15.	1.72	-8.	1.44
7	9.	-24.	1.66	-23.	1.49
8	-11.	39.	1.82	43.	1.59
9	9.	-48.	1.75	-42.	1.54
10	-9.	22.	1.65	41.	1.41
11	13.	-62.	1.67	52.	1.73
12	6.	-15.	1.72	-17.	1.45
13	-1.	5.	1.67	3.	1.57
14	-2.	64.	1.69	41.	1.66
15	5.	-26.	1.60	-36.	1.52
16	-7.	38.	1.52	18.	1.40
17	-1.	34.	1.59	54.	1.59
18	-9.	53.	1.70	65.	1.49
19	-4.	51.	1.57	60.	1.51
20	7.	-39.	1.62	-54.	1.51
21	11.	-18.	2.05	9.	1.66
22	-6.	25.	1.63	2.	1.54
23	3.	-13.	1.54	65.	1.49
24	-5.	69.	1.52	39.	1.41
25	-1.	6.	1.49	-81.	1.48
26	-8.	22.	1.73	28.	1.47
27	-7.	36.	1.64	28.	1.52
28	-3.	24.	1.42	-61.	1.42
29	-2.	28.	1.53	-69.	1.52
30	4.	-24.	1.50	-83.	1.48
31	-11.	39.	1.72	49.	1.47
32	13.	-33.	1.85	-21.	1.57
33	1.	-7.	1.39	75.	1.39
34	1.	77.	1.49	53.	1.49
35	-12.	41.	1.80	48.	1.44
36	11.	-40.	1.64	-62.	1.39
37	0.	-85.	1.52	-76.	1.47
38	-5.	72.	1.84	71.	1.62
39	-5.	24.	1.42	8.	1.32
40	5.	-13.	1.85	-12.	1.61
41	12.	-32.	1.79	-19.	1.46
42	2.	-84.	1.67	81.	1.53
43	5.	-69.	1.79	-50.	1.54
44	5.	-77.	1.75	-75.	1.50
45	10.	-54.	1.71	-35.	1.45
46	-2.	4.	2.08	17.	1.43
47	6.	-13.	1.68	-7.	1.48
sample number	yz plane				
	str°	ϕmean°	Rfhm	θmean°	Rihm
1	5.	-36.	1.51	-40.	1.46
2	1.	-66.	1.40	-16.	1.40
3	-5.	12.	1.75	10.	1.51

4	-3.	20.	1.52	15.	1.49
5	-1.	63.	1.34	-17.	1.34
6	-6.	26.	1.41	-41.	1.34
7	5.	-37.	1.49	72.	1.45
8	12.	-35.	1.75	-59.	1.54
9	11.	-38.	1.78	-36.	1.52
10	7.	-27.	1.74	-41.	1.59
11	-4.	19.	1.62	19.	1.52
12	4.	-7.	1.71	2.	1.52
13	0.	-1.	1.99	-10.	1.45
14	-7.	9.	2.03	14.	1.45
15	-6.	9.	1.84	6.	1.48
16	-7.	21.	1.65	-14.	1.53
17	5.	-50.	1.66	-47.	1.62
18	16.	-41.	2.09	-41.	1.54
19	1.	-6.	1.49	82.	1.47
20	-11.	25.	1.87	32.	1.47
21	-3.	75.	1.62	65.	1.51
22	-2.	80.	1.53	-18.	1.53
23	-13.	15.	2.12	15.	1.40
24	9.	-23.	1.71	-33.	1.52
25	1.	-5.	1.74	-21.	1.61
26	4.	-54.	1.44	-3.	1.41
27	-1.	0.	1.53	-35.	1.53
28	-6.	12.	1.57	-29.	1.48
29	-3.	9.	1.54	90.	1.44
30	-2.	42.	1.54	32.	1.52
31	1.	-6.	1.41	79.	1.40
32	8.	-48.	1.64	-51.	1.45
33	-2.	59.	1.52	55.	1.49
34	3.	-75.	1.62	-64.	1.51
35	-1.	80.	1.54	-61.	1.54
36	-2.	11.	1.44	-37.	1.44
37	-1.	9.	1.56	54.	1.53
38	10.	-46.	1.76	-42.	1.53
39	5.	-64.	1.45	-68.	1.36
40	3.	-42.	1.44	59.	1.42
41	-4.	7.	1.87	11.	1.54
42	-3.	10.	1.68	-4.	1.60
43	-3.	3.	2.05	-15.	1.51
44	-3.	8.	1.76	14.	1.55
45	0.	86.	1.50	71.	1.46
46	-4.	35.	1.51	-85.	1.48
47	0.	59.	1.50	14.	1.51

sample	zx plane				
number	str°	ϕ mean°	Rfhm	θ mean°	Rihm
1	-11.	47.	1.72	41.	1.49
2	-9.	19.	1.84	5.	1.50
3	-7.	19.	1.86	17.	1.60
4	-7.	29.	1.62	17.	1.50
5	-3.	15.	1.50	-19.	1.44
6	-9.	24.	1.70	21.	1.53
7	5.	-54.	1.48	-22.	1.45
8	0.	-11.	1.38	23.	1.38
9	-3.	16.	1.54	-62.	1.53
10	2.	-46.	1.51	-7.	1.51
11	3.	-63.	1.67	-55.	1.62
12	2.	-12.	1.44	15.	1.40

13	-2.	75.	1.53	-68.	1.52
14	6.	-72.	1.78	-60.	1.49
15	-6.	22.	1.65	7.	1.49
16	1.	-75.	1.32	-75.	1.31
17	2.	-11.	1.50	35.	1.48
18	1.	-1.	1.65	49.	1.63
19	2.	-22.	1.54	22.	1.53
20	3.	-14.	1.58	14.	1.53
21	-3.	9.	1.64	85.	1.58
22	3.	-20.	1.61	-41.	1.55
23	1.	-81.	1.49	-63.	1.45
24	-1.	16.	1.49	14.	1.47
25	-9.	34.	1.72	37.	1.53
26	-3.	5.	1.71	-8.	1.53
27	0.	0.	1.70	9.	1.53
28	2.	-76.	1.45	18.	1.43
29	1.	-22.	1.46	67.	1.45
30	-8.	30.	1.75	56.	1.62
31	-6.	13.	1.79	12.	1.60
32	-2.	9.	1.63	-2.	1.55
33	3.	-15.	1.56	-47.	1.48
34	-3.	34.	1.58	57.	1.55
35	5.	-11.	1.69	-20.	1.50
36	0.	1.	1.49	-17.	1.35
37	5.	-73.	1.78	-68.	1.48
38	1.	-9.	1.50	-45.	1.49
39	-7.	19.	1.51	-16.	1.37
40	-3.	11.	1.78	19.	1.56
41	-3.	62.	1.42	-47.	1.41
42	3.	-16.	1.67	-23.	1.59
43	1.	-29.	1.42	0.	1.42
44	2.	-65.	1.46	49.	1.44
45	-1.	2.	1.71	-6.	1.44
46	3.	-72.	1.56	-51.	1.50
47	5.	-22.	1.62	24.	1.57

Dieterich and Carter (1969) said that the *XY* plane becomes to be parallel to the cleavage plane at limb of the isoclinal fold of the multilayer fold system. On the contrary, the *XY* plane and cleavage plane are obviously oblique each other when bulk strain is not so large and the viscous contrast is great between layer and matrix in the single layer system. Thus, the relation between cleavage plane and the *XY* plane of strain ellipsoid is important, but we cannot correlate the numerical experimental results obtained by Dieterich and Carter (1969) with the large scale natural folds, because we found no cleavages in the homoclinal part which is the limb part of the large scale fold in the area.

(2) The strain value obtained by the strain analysis using quartz grain marker is small compared with that of the other folded area, for example, the Alps. The principal value of strain ellipsoid is much smaller than the value expected from the geological structure (Hayashi,1988,1989). One of the reason is a large competency contrast between folded layer and matrix. The reason of small strain value does not depend on the nonconsolidation of strata that Hayashi (1988,1989) forecasted, because the *XY* plane of strain ellipsoid is roughly disposed parallel to the bedding and so the *XY* plane reflects deformation. If the strata is soft and not yet consolidated, quartz grains are not deformed but only rotated. The strata of so called Shimanto type alternation of sandstone and mudstone like the Kayo Formation was suffered tectonic movement under the consolidated condition. We

Table 8. Values of the averaged initial ellipse. *size* : sample size. R_i : axial ratio of the averaged initial ellipse. Φ ($\equiv$ | θ -α |) : absolute value of the difference from the direction of the long axis of the averaged initial ellipse and the long axis of strain ellipse.

sample	xy plane			yz plane			zx plane		
number	size	$\bar{R}_i$	Φ°	size	$\bar{R}_i$	Φ°	size	$\bar{R}_i$	Φ°
1	64	1.00306	1.	74	1.00066	89.	69	1.00064	89.
2	57	1.00360	0.	54	1.00285	0.	53	1.00293	89.
3	53	1.00279	0.	80	1.00005	16.	60	1.00141	1.
4	68	1.00325	0.	75	1.00154	1.	62	1.00111	1.
5	61	1.00464	0.	49	1.00002	1.	59	1.00222	0.
6	39	1.00272	0.	54	1.00205	0.	60	1.00323	89.
7	62	1.00083	2.	70	1.00207	90.	59	1.00189	0.
8	56	1.00112	1.	62	1.00282	90.	60	1.00278	0.
9	86	1.00232	89.	78	1.00219	90.	68	1.00087	0.
10	70	1.00285	0.	70	1.00011	6.	72	1.00222	0.
11	68	1.00288	1.	66	1.00103	90.	78	1.00264	0.
12	71	1.00196	89.	80	1.00119	1.	68	1.00248	90.
13	79	1.00114	0.	83	1.00266	1.	79	1.00333	90.
14	83	1.00151	0.	73	1.00102	2.	89	1.00204	90.
15	91	1.00157	90.	79	1.00207	89.	72	1.00021	6.
16	66	1.00059	90.	69	1.00074	90.	69	1.00226	90.
17	58	1.00258	0.	46	1.00100	90.	56	1.00241	90.
18	56	1.00045	3.	60	1.00208	0.	74	1.00214	90.
19	62	1.00251	0.	60	1.00125	90.	72	1.00064	90.
20	78	1.00046	1.	54	1.00285	90.	54	1.00080	89.
21	56	1.00182	89.	75	1.00335	0.	63	1.00038	3.
22	75	1.00240	90.	66	1.00203	90.	64	1.00359	0.
23	69	1.00250	0.	51	1.00088	1.	63	1.00122	90.
24	66	1.00039	88.	78	1.00142	89.	57	1.00418	0.
25	66	1.00041	2.	54	1.00325	0.	56	1.00265	0.
26	53	1.00201	0.	60	1.00143	0.	49	1.00025	3.
27	63	1.00188	90.	72	1.00083	90.	61	1.00121	1.
28	60	1.00400	90.	69	1.00253	0.	53	1.00045	90.
29	59	1.00386	0.	53	1.00322	90.	67	1.00349	0.
30	54	1.00128	89.	36	1.00404	0.	52	1.00246	0.
31	45	1.00014	88.	59	1.00262	90.	42	1.00121	90.
32	46	1.00210	0.	37	1.00353	0.	41	1.00053	89.
33	37	1.00180	0.	43	1.00046	1.	41	1.00078	89.
34	48	1.00366	0.	60	1.00006	7.	45	1.00150	90.
35	69	1.00005	23.	61	1.00461	0.	63	1.00041	0.
36	70	1.00086	90.	57	1.00009	4.	70	1.00083	1.
37	77	1.00353	0.	65	1.00098	0.	62	1.00133	89.
38	64	1.00042	4.	70	1.00087	88.	57	1.00080	1.
39	62	1.00024	4.	64	1.00173	90.	71	1.00280	90.
40	54	1.00306	90.	78	1.00035	89.	80	1.00211	0.
41	93	1.00269	89.	75	1.00099	1.	65	1.00099	90.
42	90	1.00265	0.	62	1.00104	1.	74	1.00118	90.
43	74	1.00100	0.	80	1.00215	1.	78	1.00297	0.
44	105	1.00130	1.	79	1.00029	85.	60	1.00329	0.
45	80	1.00323	89.	72	1.00042	0.	90	1.00100	1.
46	66	1.00266	0.	72	1.00121	90.	73	1.00089	1.
47	63	1.00329	90.	90	1.00162	90.	91	1.00241	0.

wonder why the value of ε_s takes always around 0.2 (0.1-0.5) when we analyze the strain using the quartz grain as strain marker. The value of ε_s shows similar quantity to that obtained from the sample of the metasediments collected from the Midland zone in the Nepal Himalaya. The parameter ε_s is the amount of strain defined by Nadai (1963), and is the value multiplied the octahedral unit shear γ_{oct} by $\frac{\sqrt{3}}{2}$. We consider that the reason of low ε_s value depends on the competency contrast.

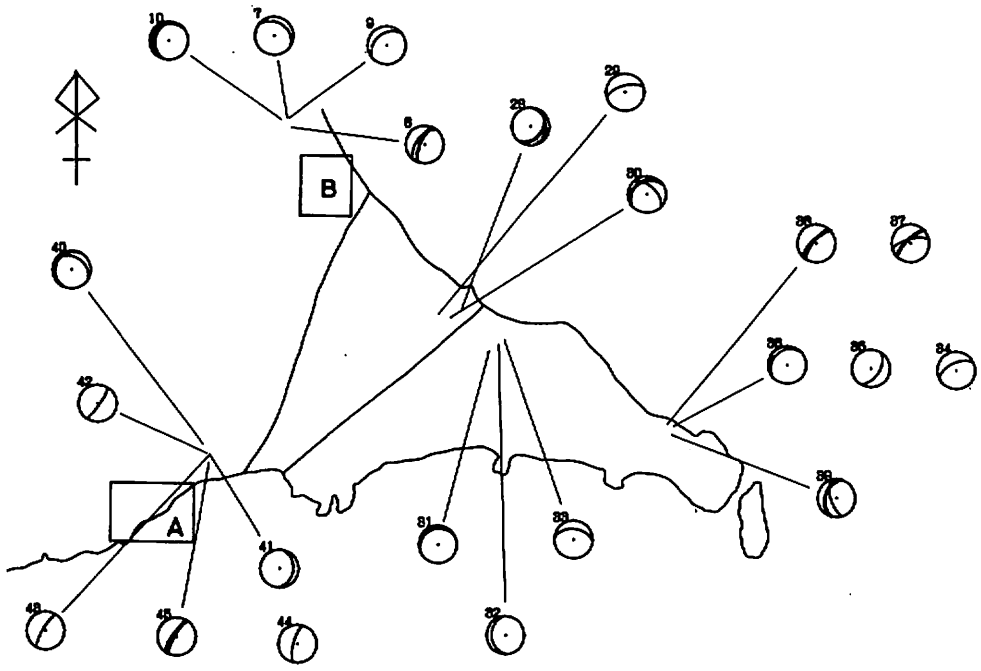

Fig. 17. Distribution map of *XY* plane and bedding plane. The *XY* plane and bedding plane are illustrated as a great circle projected to the lower hemisphere of the Schimdt net. Thin drawn great circle is the *XY* plane. Thick drawn great circle is the bedding plane. Not all the diagrams show both the great circles because of the lack of data of bedding plane.

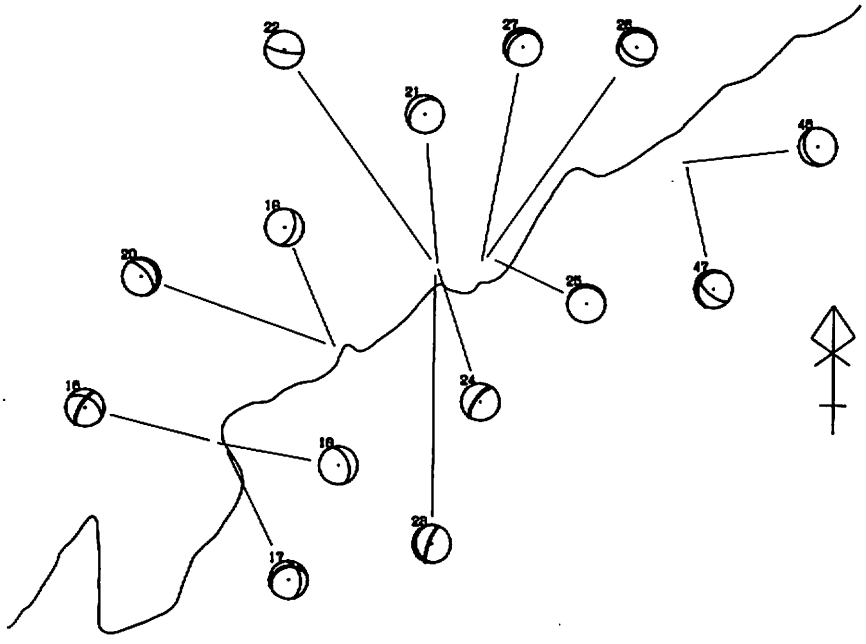

Fig. 18. Distribution map of *XY* plane and bedding plane in the area A.

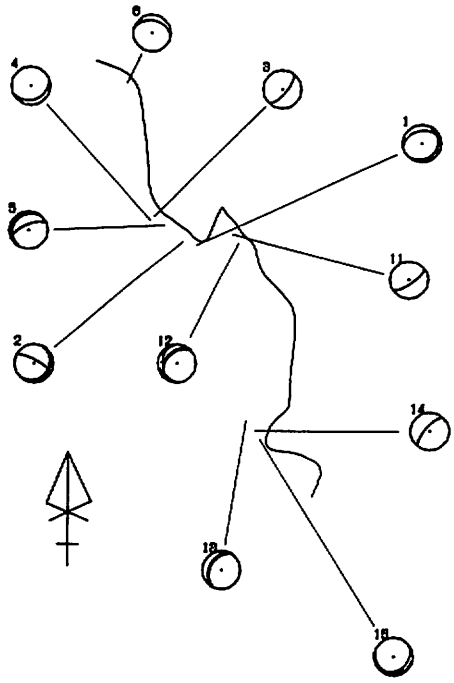

Fig. 19. Distribution map of *XY* plane and bedding plane in the area B.

(3) We do not recognize clear negative relationship between the axial ratio $\acute{R}_i$ of averaged initial ellipse and the sample size, which are expected by the theoretical consideration after Shimamoto and Ikeda (1976).

References

Davidson Jr.,D.M.,1983. Strain analysis of deformed granitic rocks (Helikian), Muskoka District, Ontario. *J. Struct. Geol.*, 5 : 181-195.

Dieterich, J. H. & N. L. Carter, 1969. Stress-history of folding. *Am. J. Sci.*, 267 :129-154.

Dunnet,D.,1969. A technique of finite strain analysis using elliptical particles. *Tectonophysics*, 7:117-136.

Dunnet,D. & A.W.B.Siddans,1971. Non-random sedimentary fabrics and their modification by strain. *Tectonophysics*,12:307-325.

Elliott,D.,1970. Determination of finite strain and initial shape from deformed elliptical objects. *Bull.Geol.Soc.Am.*, 81:2221-2236.

Fry,N.,1979. Random point distributions and strain measurement in rocks. *Tectonophysics*,60:89-105.

Fukuda,Y., A. Kaihori, H. Otsuka & S.Hayasaka, 1978. A note on the sedimentological features of the Kayo Formation in Okinawa-shima, Ryukyu Islands. Geological studies of the Ryukyu Islands (ed. by K.Kizaki),3:39-52. (in Japanese with English abstract)

Hayashi,D.,1988. Three dimensional finite strain analysis - with reference to Kayo Formation, Kunchan Group, Okinawa-jima -. *J. Geol.Soc. Japan*,94:757-768. (in Japanese with English abstract)

Hayashi,D.,1989. Correction of errors in "Three dimensional finite strain analysis - with reference to Kayo Formation, Kunchan Group, Okinawa-jima - Hayashi,1988". *J.Geol.Soc. Japan*,95:553-558. (in Japanese with English abstract)

Hayashi,D.,1992. Properties on the initial marker ellipses - in the case of the Kayo Formation, Kunchan Group, Okinawa-jima -. *J. Geol.Soc. Japan*,98:841-854. (in Japanese with English abstract)

Hayashi,D. & K. Kizaki, 1985. Middle and northern part of Okinawa-jima. In : Kizaki, K., ed. : Geology

of the Ryukyu Islands, Okinawa Taimusu Sha,:93-106. (in Japanese)

Hext,G.R.,1963. The estimation of the second-order tensors with related tests and designs. *Biometrika*, 50:353-372.

Jensen,L.N.,1984. Quartz microfabric of the Laxfordian Canisp Shear Zone,NW Scotland. *J.Struct. Geol.*,6:293-302.

Lacassin,R. & J.van den Driessche,1983. Finite strain determination of gneiss:application of Fry's method to porphyroid in the southern Massif Central (France). *J.Struct.Geol.*,5:245-253.

Lisle,R.J.,1985. Geological strain analysis ; A manual for the R_f/ϕ method. 99pp., Pergamon.

Nadai,A.,1963.Theory of flow and fracture of solids. 705pp., McGraw-Hill, New York.

Odling,N.E.,1984.Strain analysis and strain path modelling in the Loch Tollie gneisses, Gairloch, NW Scotland. *J.Struct.Geol.*,6:543-562.

Owens,W.H.,1984. The calculation of a best-fit ellipsoid from elliptical sections on arbitrarily orientated planes. *J.Struct.Geol.*,6 ; 571-578.

Peach,C.J. & R. J.Lisle,1979. A FORTRAN IV program for the analysis of tectonic strain using deformed elliptical markers. *Computers & Geosciences*,5:325-334.

Ramsay,J.G.,1967. Folding and fracturing of rocks. 568pp., McGraw-Hill.

Seno,S.,1992.Finite strain and deformation within the Brianconnais Castelvecchio-Cerisola nappe of the Ligurian Alps, Italy. *J.Struct.Geol.*,14 ; 825-838.

Shimamoto,T. & Y. Ikeda, 1976. A simple algebraic method for strain estimation from deformed ellipsoidal objects.1.Basic theory. *Tectonophysics*, 36:315-337.

Siddans,A.W.B., B. Henry, R. Kligfield, W. Lowrie, A. Hirt & M.N. Percevault, 1984. Finite strain patterns and their significance in Permian rocks of the Alpes Maritimes (France). *J.Struct. Geol.*,6 ; 339-368.

Suzuki,Y. & H. Ujiié, 1985. *Nummulites Amakusaensis* from the Kayo Formation and its significance on the Ryukyu Island Arc development. *Chikyu Kagaku*, 39:385-388.